Widespread axonal sodium channel changes with progressive disruption of the node of Ranvier integrity following experimental concussion

Przemyslaw P. McEwan[1,#], Hailong Song[1,#], Alexandra Tomasevich[1], Victoria E. Johnson[1], Jean-Pierre Dolle[1], Douglas H. Smith[1,*].

[1]Department of Neurosurgery, Center for Brain Injury and Repair, Department of Neurosurgery, University of Pennsylvania, Philadelphia, PA 19104, USA;

[#]These authors equally contributed to this work.

***Corresponding Author**
Dr. Douglas H. Smith
Department of Neurosurgery, Center for Brain Injury and Repair, University of Pennsylvania, Philadelphia, PA 19104, USA
E-mail: smithdou@pennmedicine.upenn.edu
Address: 3320 Smith Walk, 105 Hayden Hall
Phone: 215-573-3156
Fax: 215-573-3808

Acknowledgement
This research was made available with the support from National Institutes of Health grants R01NS092398, R01NS038104, R01NS094003, R01EB021293, Paul G. Allen Family Foundation, and the PA Consortium on Traumatic Brain Injury 4100077083 (all to D.H.S). Here, we thank Dr. Stephen Waxman from Yale University, Dr. Matthew Rasband from Baylor College of Medicine, and Dr. Peter Brophy from The University of Edinburgh for providing primary antibodies used in this study. The funders had no role in study design, data collection and analysis, decision to publish, or preparation of the manuscript.

Abstract
Although concussion is a major health concern, little is known about pathophysiological changes that cause post-traumatic cognitive dysfunction. Nonetheless, emerging evidence suggests that selective damage to white matter axons, or diffuse axonal injury (DAI), disrupts brain network connectivity and function. While voltage gated sodium channels (VGSCs) and their anchoring proteins at the nodes of Ranvier (NOR) on axons are key elements of the brain's network signaling machinery, potential changes in their integrity has not been studied in context with DAI. Here, we utilized a well-characterized and clinically relevant swine model of concussion that induces evolving swollen axonal profiles, demonstrated by amyloid precursor protein accumulation (APP) across the white matter. With this model, we found widespread loss of VGSC isoform 1.6 (Nav1.6) concurrent with progressive disruption of NOR cytoskeleton proteins on axons in close proximity, yet distinct from APP+ swollen axonal profiles in the same white matter tracts. Accordingly, these features may represent a unique newfound phenotype of axonal pathology in DAI. These changes persisted 2 weeks after injury and included increases in NOR length and the appearance of amorphous and void nodes as well as heminodes. In addition, there was also a distinct loss in expression of proteins that together serve as major NOR anchoring scaffolds, including βIV-spectrin, ankyrin G, and neurofascin, which were found diffusing into paranodal spaces. Collectively, this widespread and progressive disruption of VGSCs and NOR could have important implications for mechanisms underlying brain network dysfunction after concussion.

Key Words: concussion, diffuse axonal injury, voltage gated sodium channel isoform 1.6, node of Ranvier, βIV-spectrin, ankyrin G, and neurofascin.

Introduction

Concussion has recently been recognized as a major health issue, with over 2 million cases occurring in the US each year [12]. Although this disorder is alternatively referred to as 'mild' traumatic brain injury (TBI), this designation is somewhat of a misnomer considering that more than 15% of individuals with concussion endure persisting neurocognitive dysfunction [25]. While the presence of chronic symptoms suggests that concussion can induce long-lasting or permanent damage to the brain, there is as yet no consensus regarding its evolving pathophysiological underpinnings [41]. Nonetheless, emerging evidence suggests that structural and physiological disruption of brain networks is an important substrate of concussion. In particular, selective damage to axons across the white matter, referred to as diffuse axonal injury (DAI), is increasingly endorsed as a key contributor to the acute and chronic clinical manifestations of concussion [6, 21, 30]. It is thought that DAI impairs the normal flow of information across brain networks, leading to classical concussion symptoms such as delayed processing speed [32]. This premise is supported by studies of severe TBI in humans, where white matter injury and specifically DAI has been implicated in slowed information processing [13, 24].

Several lines of evidence implicate axonal sodium channels as playing an important role in network dysfunction after TBI. Studies using rodent models of TBI have shown compromised action potential (AP) generation and axonal conduction defects of white matter after injury [4, 28]. In addition, experimental TBI was shown to reduce the amplitude of waveforms of evoked compound APs across the corpus callosum, suggesting inefficient AP firing and transduction across the white matter [37]. Since voltage-gated sodium channels (VGSCs) are essential in AP generation and managing rate of discharge [5, 9], damage and/or changes in expression of VGSCs due to injury could play a key role in dysfunctional signaling across brain networks. This is supported by studies using an *in vitro* model of dynamic stretch injury of micropatterned unmyelinated axonal tracts [31, 46]. This injury was found to selectively induce non-inactivation of VGSCs, resulting in the massive influx of sodium, in turn, leading to calcium influx, calcium-activated proteolytic damage to VGSCs and a change in VGSC expression [17, 43, 44]. However, the *in vivo* molecular and temporal changes of VGSCs among myelinated axons underlying DAI after concussion is not known.

Along with VGSCs, the integrity of the nodes of Ranvier (NOR) on myelinated axons is also essential for network function. In normal conditions, signals generated at the axon initial segment (AIS) are propagated down the axonal length via saltatory conduction directed by the NORs [33]. In particular, initial AP induction relies on synchronized activity primarily on high density clustering of the VGSC isoform 1.6 (Nav1.6) at the NORs [2, 35, 39]. Such clustering and distribution of VGSCs within NOR is largely dependent on their binding with βIV-spectrin as well as interaction with a cytoskeletal complex of ankyrin G (AnkG) and neurofascin (Nfasc) that collectively mediate nodal integrity [11]. Notably, brain injury in rodent models induces abnormal organization of NORs, which plays a role in dysfunctional AP generation [28, 42]. However, little is understood regarding potential morphological changes of NOR cytoskeleton integrity as a whole and how it affects Nav1.6 composition at NOR after concussion.

To investigate the effects of concussion on Nav1.6 and NOR integrity, we used a well-characterized swine model of head rotational acceleration utilizing parameters that are based on human concussion biomechanics [8, 10]. Importantly, due to the relatively large gyrencephalic nature of the swine brain with large white matter domains, this model induces DAI that is identical in appearance to human DAI [10]. Following experimental concussion with this model, we examined temporally evolving changes in Nav1.6 expression as well as the morphological integrity of NOR cytoskeleton.

Materials and methods

Experimental design

A total of 13 female miniature swine (Hanford strain, Sinclair Research Center, Inc., Columbia, MO), weighing 22-25 kg and 6-7 months old were included in the current study, as signatures of DAI well characterized in previous studies [8, 10, 22, 23]. All animal experiments were conducted in accordance with protocols approved by the Institutional Animal Care and Use Committee at the University of Pennsylvania. Animals were divided in groups, including survival after injury of 6 hours (hrs) (n=3), 72 hrs (n=3), and 2 weeks (wks) (n=3) in comparison to sham animals (n=4). Here, we hypothesized that rapid rotational acceleration injury will cause widespread and progressive Nav1.6 and NOR integrity changes. The proposed animal number was expected to provide significant statistical power, considering absence of DAI in sham control animals.

Animal preparation and rotational acceleration model of concussion

The animal preparation was carried out as previously described [8, 10, 22, 23]. Briefly, prior to surgical procedures, animals were fasted for over 12 hrs. Anesthesia was induced by IM administration of midazolam (0.4mg/kg) followed by 2-5% Isoflurane gas via snout mask, followed by intubation and anesthesia maintaining on a surgical plane via 2.5% isoflurane. Animals' status were monitored and documented throughout the procedure.

Parameters for experimental concussion were scaled to mimic the biomechanics of human concussion and have previously been characterized to produce DAI [8, 10, 22, 23]. The animals' heads were secured on to a padded linkage assembly connected to the HYGE device. The HYGE device is a pneumatic actuator capable of converting linear motion to angular (rotational) motion to produce impulsive head rotation of 110 degree in the coronal plane in 20 ms. During the injury, the center of rotation was adjusted close to the brain's center of mass. The peak angular velocity attained during the injury ranged between 225 to 250 rad/s. All the rotational kinematics were recorded by using angular velocity transducers (Applied Technology Associates).

After the injury induction, the animal's head was immediately released from the clamp. The animals were monitored continuously in the housing facility until they recovered from anesthesia. Preemptive analgesia of 0.1-0.3 mg of Buprenex (sustained release) SQ and acetaminophen 50 mg/kg PR were provided post injury. Sham animals underwent all procedures described above except for head rotation. All of the experimental designs and protocols were approved by the University of Pennsylvania Institutional Animal Care and Use Committee, and animal experiments were carried out in accordance with the NIH Guide for the Care and Use of Laboratory Animals.

Tissue Preparation

Both injured and sham control animals were euthanized at the post injury time points noted above as well as previously described [22, 23]. Briefly, transcardial perfusion was performed under surgical plane anesthesia using heparinized saline (2L) followed by 10 % neutral buffered formalin (NBF) (8L). The brain was removed, extracted, and post-fixed in 10% NBF for 7 days. Further, the brains were blocked into 5 mm coronal sections for gross examination. The tissue blocks were then processed for standard paraffin embedding in an automated tissue processor (Shandon Scientific Instruments, Pittsburgh, PA). Serial sections (8 µm) were cut on a Leitz rotary microtome (Leica, Malvern, PA). The sections were mounted on Fisherbrand Superfrost/Plus microscope slides (Fisher Scientific, Pittsburgh).

Immunohistochemical (IHC) staining and quantification

Standard immunohistological techniques were performed as described [22, 23]. For IHC staining, tissue sections were first deparaffinized by baking at 60 ºC and passing through two changes of xylene, followed by rehydration. Sections were then immersed in hydrogen peroxide for quenching endogenous peroxidase activity. Antigen retrieval was carried out by microwaving

in Tris EDTA buffer. Next, slides were blocked using 50µl normal horse serum (Vector Labs, Burlingame, CA) per 5ml of Optimax buffer (BioGenex, San Ramon, CA) at room temperature (RT) for 30 mins. Sections were incubated with primary antibody (amyloid precursor protein (APP) (Millipore Sigma, MAB348, 1:80,000) overnight at 4 ºC (**Table 1**). After rinsing in PBS, the sections were probed with the appropriate biotinylated secondary antibody (Vector Labs, Burlingame, CA) for 30 mins at RT, followed by avidin biotin complex incubation. Visualization was made by DAB peroxidase substrate kit (Vector Labs, Burlingame, CA) and counterstaining using hematoxylin. Images were acquired at automated high-resolution scanning (20x) using the Aperio ScanScope and annotation of APP positive DAI profiles was performed by Aperio ImageScope software (Leica Biosystems, Wetzlar, Germany).

Quantitative analyses were performed blind to the injury status, as previously reported [22]. For quantification, APP positive swollen axonal profiles within corpus callosum and periventricular white matter from each swine were counted and quantified as the average number of profiles per unit area (μm^2), then computed for statistical analysis.

Immunofluorescent (IF) staining and quantification

For IF staining, similar procedures were followed as IHC without hydrogen peroxide quenching. Overnight 4 ºC primary antibody incubation were performed using Nav1.6 (Alomone Labs, ASC-009, 1:200), Caspr (from Stephen Waxman, Yale University, 1:1,000), APP (Millipore, MAB348, 1:8,000), βIV-spectrin (from Matthew Rasband, Baylor College of Medicine, 1:1,000), AnkG (NeuroMab, N106/36, 1:1,000), and Neurofascin (Nfasc) (from Peter Brophy, The University of Edinburgh, 1:2,000) (**Table 1**), followed by a corresponding Alexa Fluor secondary antibody (ThermoFisher, 1:250) for 60 mins at RT. The IF images were acquired and viewed using a Leica SP5 confocal microscope (Leica, Germany).

For IF quantification, two investigators performed the imaging analysis were blinded to the animal treatment groups. The nodal fluorescent intensities of Nav1.6, βIV-spectrin, and Nfasc were measured using ImageJ and their relative ratios were compared among groups. Specifically, the fluorescent intensity of markers within one NOR was measured individually and averaged for a region of interest (ROI). The averaged fluorescent intensity from each ROI was used for statistical analysis comparing among different groups. Caspr (contactin-associated protein) staining labeled septate-like paranodal space [38], and therefore used for measuring NOR length and characterizing NOR morphologies, including amorphous (clustered or misshapen Caspr and NOR domains), void (paired Caspr domain in the absence of NOR), and heminodes (unpaired Caspr domain). The percentage of various nodal morphologies was calculated by dividing the total number of NOR observed. Finally, βIV-spectrin and AnkG diffusion was calculated based upon its paranodal IF intensities and compared among groups.

Statistical Analysis

Statistical analysis was performed using GraphPad Prism statistical software (GraphPad Software Inc. La Jolla, CA). Violin plot was used to illustrate the statistical differences as well as the frequency distribution of the data (dashed lines indicated median and quartiles). One-way ANOVA were used to determine differences between groups. P values of post hoc tests for multiple comparisons were adjusted using the Tukey test. A p value less than 0.05 was considered significant for all analyses, with * indicating $p<0.05$, ** for $p<0.01$, *** for $p<0.001$, and **** for $p<0.0001$.

Results

Progression of DAI after experimental concussion

Examination of DAI was performed using APP IHC as a key marker capturing characteristic swollen axonal profiles due to mechanical rupture of axon cytoskeleton. Indeed, widespread APP positive profiles were observed at 6hrs, 72hrs, and 2wks post injury (**Fig. 1A-**

1B). No APP positive axon was seen in sham control animals. Mapping of APP accumulations revealed its multifocal distributions particularly at periventricular white matter and corpus callosum, as previously characterized and close to those observed in human DAI [8, 22]. Specifically, 72hrs post injury showed the highest numbers of APP positive swollen axons, indicating peak DAI captured (**Fig. 1C**). Such axonal profiles were displayed as terminal swelling, beading, and fusiform profiles (**Fig. 1D**), suggesting multiple axonal transport disruption. Further, evident axonal bulbs were identified, particularly at periventricular white matter, implying disconnection of axons due to injury.

Widespread loss of Nav1.6 and progressive disruption of NOR integrities associated with DAI

As VGSC dysregulation and proteolysis have been observed in an *in vitro* model of traumatic axonal injury [17, 19, 46] , here, we investigated potential changes in an isoform specific VGSC Nav1.6 at NOR in relation to DAI (marked by APP) after concussion in swine. Caspr was used to visualize paranodal space. Specifically, widespread Nav1.6 changes were observed in close proximity to, yet distinct from APP positive swollen axonal profiles up to 2wks post injury (**Fig. 2A**). Interestingly, acute decreases of Nav1.6 expression within NOR were primarily identified at 6hrs and 72hrs post injury (**Fig. 2B-2C**), suggesting compromised AP transduction along myelinated axons acutely after concussion.

Since Nav1.6 is mainly clustered and distributed within NOR, we further examined whether such Nav1.6 changes were corresponded to compromised NOR integrities. Indeed, as opposed to the normal NOR characterized by paranodal Caspr and nodal Nav1.6 expression, various changes in NOR structural organizations, including amorphous, void, and heminode morphologies, were captured from 6hrs to 2wks after concussion (**Fig. 3A**). The percentages of those abnormal NOR profiles were progressively elevated after injury and relevant to APP positive swollen axonal profiles (**Fig. 3B-3D**). Concurrently, significant increases of NOR lengths were also found (**Fig. 3E**). Such changes in NOR length and NOR phenotypes may be responsible for a slower AP conduction speed underlying DAI [3, 14].

Changes in NOR mediated by its cytoskeleton scaffold alterations after concussive injury

To further understand the structural basis for NOR changes after concussion, both βIV-spectrin and AnkG, as the major cytoskeleton scaffold critical for maintaining its ultrastructure [34], were investigated (**Fig. 4A**). Although βIV-spectrin expression level was not altered, a significant increase in βIV-spectrin void node percentage was identified at 6hrs post injury (**Fig. 4B-4C**). Intriguingly, evident βIV-spectrin diffusions into the paranodal space peaking at 72hrs were found (**Fig. 4D-4E**). Interesting, a widespread loss of AnkG expression, that serving as an anchor scaffold for Nav1.6, within NOR were persisted at 2wks (**Fig. 5A-5B**). Similarly, a concurrent progressive AnkG paranodal diffusion were seen at 6hrs post injury (**Fig. 5C**).

Besides above cytoskeletal proteins, NOR also contains a rich extracellular matrix that bind with complex adhesion molecules, including Nfasc [26, 40]. In particular, Nfasc is important for regulating Nav1.6 clustering and maintenance [1]. Interestingly, significant loss of nodal Nfasc expression was found both at 6hrs and 72hrs post injury (**Fig. 6A-6B**), with no change regarding its paranodal localizations. Such decreases in Nfasc profiles were also associated with significant elevations in the percentages of Nfasc void node (**Fig. 6C**). Together, these data imply that the acute loss of Nav1.6 and NOR integrities could be explained by an acute destabilization along with reorganization of NOR-paranodal complex structures after experimental concussion.

Discussion

Using a clinically relevant swine model of concussion, we observed widespread and progressive changes in the expression and distribution of Nav1.6 on white matter axons along with progressive disruption of NOR morphologies and its structural integrity (**Fig. 7**). Adjacent to, but distinct from swollen axonal profiles, these findings represent a newfound phenotype of axonal pathology as an additional feature of DAI that may play a key role in concussion symptoms. Indeed, considering that Nav1.6 and NOR govern signal generation and flow of information [3, 14, 15], extensive disruption of both across the white matter provides a potential mechanistic basis that underlies brain network dysfunction after concussion.

Although there is not yet consensus, it has long been suspected that DAI in plays an important role in concussion [21, 41]. In 1994, a seminal post-mortem study of concussion in humans who died shortly after injury from other causes, identified DAI as the only neuropathologic change [7]. In addition, selective axonal pathology has been observed in multiple animal models of concussion [20, 21]. Axons are thought to be particularly vulnerable to damage from the mechanical forces of concussion due to their high organization in white matter tracts and their uniquely long and delicate ultrastructure [29]. In concussion, brain tissue deformation during head rotational acceleration can damage axonal microtubules causing interruption of axonal transport and accumulation of proteins in swollen axonal profiles. Due to its high abundance in axons, APP immunohistochemistry has become the ‘gold standard’ method to evaluate axonal swellings and diagnose DAI. However, in human TBI and the swine model of concussion, we recently found that other axonal proteins and protein fragments accumulate in axon swellings, that surprisingly do not colocalize with APP [22]. This suggests that there are multiple phenotypes of axonal swellings in DAI that may represent distinct pathways of axonal transport interruption.

The current data identifies another unique and newfound phenotype of axonal pathology that occurs in the absence of overt axonal transport interruption. Specifically, changes nodal sodium channel expression and distribution of NOR integrity were identified on axons that did not display protein accumulation in swollen axonal profiles. In addition, while APP+ axonal swellings and axons demonstrating sodium channel and NOR changes were often found nearby in the same white matter tracts, the latter were more numerous and more diffusely distributed across the white. Furthermore, while the extent of APP+ axonal swellings leveled off or decreased over time, the sodium channel and NOR pathological changes appeared to progress to at least two weeks post-concussion. Since these sodium channel and NOR changes appear to occur in the absence of apparent transport interruption or evidence of degeneration as compared to APP+ swollen axons, this may represent a milder phenotype of axon pathology. Nonetheless, these pathological changes represent widespread disruption of the signaling machinery on axons, which could play an important role in network dysfunction and loss of connectivity of the white matter. While these observations expand the spectrum of pathophysiological processes that comprise DAI in concussion, future studies are needed to better understand how multiple phenotypes of axonal pathology can occur for axons in the same tract that were exposed to the same mechanical loading and how different phenotypes of axonal pathology affect function.

Previous studies of traumatic axonal injury have implicated mechanical and proteolytic damage to VGSCs. *In vitro* studies of dynamic stretch of micropatterned unmyelinated axon tracts demonstrated massive calcium influx after injury [17, 43, 46]. This was found to be a downstream consequence of sodium channel non-inactivation causing sodium influx, reversal of the sodium-calcium exchanger and activation of voltage-gated calcium channels. In turn, the high calcium levels were shown to activate calpain, leading to proteolytic cleavage of VGSCs and loss of immunoreactive signal in protein chemistry studies [43, 44]. Similarly, in the present study, by 6hrs post-concussion, there was a decrease in density of immunoreactive Nav1.6 at

NOR within corpus callosum and periventricular white matter. This may indicate that a similar proteolytic degradation of sodium channels of myelinated axons occurs in concussion as was found *in vitro*.

Focused analysis of NOR further revealed several changes encompassing progressive disruption of the NOR cytoskeletal and adhesion molecules associated with pathological changes in morphology. Normal organization, morphology and function of NOR highly depends on βIV-spectrin working together with AnkG to secure a high density of nodal Nav1.6 in myelinated axons [16, 27]. Indeed, study has shown that recruitment of βIV-spectrin to NOR in mice was dependent on AnkG [18]. This specific architecture is essential for the generation of APs and their propagation down the axon via salutatory conduction. However, following concussion in the present study, we found persistent diffusion of βIV-spectrin and AnkG into the paranode and the progressive appearance of void nodes. These findings are consistent with a previous analysis of NOR following TBI in a rat model, where calpain was shown to degrade αII-spectrin and AnkG in the white matter suggesting the nodal cytoskeletal integrity was disrupted [36].

Further, the loss of NOR ultrastructure following concussion in swine resulted in morphological changes that included clustered or misshapen nodal and paranodal spaces. Many of these amorphous nodes were defined as void or blank due the remarkable absence of Nav1.6 signal, which may reflect the loss of tethering by AnkG to the nodal space, potentially due to proteolysis. Likewise, concussion induced the appearance of heminodes, characterized as having only one Caspr positive paranode without its flanking partner on the opposite side of the node, demonstrating further disruption of the nodal and paranodal architecture. These amorphous nodes may be similar to those described in a recent study showing ultrastructural changes to NOR and an increase in heminodal length at 3 days post concussive TBI in mice [28].

Another important ultrastructural component of NOR is Nfasc, which is essential for clustering of AnkG and general maintenance of nodal integrity [26, 40]. This is essential as mice lacking nodal Nfasc die at postnatal day 7 due to severely diminished brain signaling [40]. Following concussion in swine, there was a significant reduction of Nfasc immunoreactivities within the nodal gap. In addition, there was an increasing number of Nfasc void nodes at 6 and 72 h following concussion.

Collectively, these data identify a new axonal pathology phenotype of widespread disruption of the nodal cytoskeleton and loss of Nav1.6 across the white matter following concussion in swine. This trauma-induced channelopathy may represent a mechanism underlying disruption of brain circuitry that was demonstrated in a recent electrophysiological study using the same model [45]. These findings warrant further studies to explore how this channelopathy may play a role in network and cognitive dysfunction after concussion.

Author contributions

Designed research: Przemyslaw P. McEwan, Hailong Song, and Douglas H. Smith. Performed research: Przemyslaw P. McEwan, Hailong Song, Alexandra Tomasevich, and Douglas H. Smith. Analyzed data: Przemyslaw P. McEwan, Hailong Song, Alexandra Tomasevich, Victoria E. Johnson, and Douglas H. Smith. Wrote the paper: Przemyslaw P. McEwan, Hailong Song, and Douglas H. Smith, with significant scientific inputs from Jean-Pierre Dolle. All authors reviewed and approved the current version of the manuscript.

Compliance with ethical standards

All applicable international, national, and/or institutional guidelines for the care and use of animals were followed.

Conflict of interest

The authors have no conflicts of interest to declare that are relevant to the content of this article.

References

1 Amor V, Feinberg K, Eshed-Eisenbach Y, Vainshtein A, Frechter S, Grumet M, Rosenbluth J, Peles E (2014) Long-term maintenance of Na+ channels at nodes of Ranvier depends on glial contact mediated by gliomedin and NrCAM. J Neurosci 34: 5089-5098 Doi 10.1523/JNEUROSCI.4752-13.2014

2 Amor V, Zhang C, Vainshtein A, Zhang A, Zollinger DR, Eshed-Eisenbach Y, Brophy PJ, Rasband MN, Peles E (2017) The paranodal cytoskeleton clusters Na(+) channels at nodes of Ranvier. Elife 6: Doi 10.7554/eLife.21392

3 Arancibia-Carcamo IL, Ford MC, Cossell L, Ishida K, Tohyama K, Attwell D (2017) Node of Ranvier length as a potential regulator of myelinated axon conduction speed. Elife 6: Doi 10.7554/eLife.23329

4 Armstrong RC, Mierzwa AJ, Marion CM, Sullivan GM (2016) White matter involvement after TBI: Clues to axon and myelin repair capacity. Exp Neurol 275 Pt 3: 328-333 Doi 10.1016/j.expneurol.2015.02.011

5 Bean BP (2007) The action potential in mammalian central neurons. Nat Rev Neurosci 8: 451-465 Doi 10.1038/nrn2148

6 Benjamini D, Iacono D, Komlosh ME, Perl DP, Brody DL, Basser PJ (2021) Diffuse axonal injury has a characteristic multidimensional MRI signature in the human brain. Brain: Doi 10.1093/brain/awaa447

7 Blumbergs PC, Scott G, Manavis J, Wainwright H, Simpson DA, McLean AJ (1994) Staining of amyloid precursor protein to study axonal damage in mild head injury. Lancet 344: 1055-1056 Doi 10.1016/s0140-6736(94)91712-4

8 Browne KD, Chen XH, Meaney DF, Smith DH (2011) Mild traumatic brain injury and diffuse axonal injury in swine. J Neurotrauma 28: 1747-1755 Doi 10.1089/neu.2011.1913

9 Catterall WA (2017) Forty Years of Sodium Channels: Structure, Function, Pharmacology, and Epilepsy. Neurochem Res 42: 2495-2504 Doi 10.1007/s11064-017-2314-9

10 Cullen DK, Harris JP, Browne KD, Wolf JA, Duda JE, Meaney DF, Margulies SS, Smith DH (2016) A Porcine Model of Traumatic Brain Injury via Head Rotational Acceleration. Methods Mol Biol 1462: 289-324 Doi 10.1007/978-1-4939-3816-2_17

11 Eshed-Eisenbach Y, Peles E (2013) The making of a node: a co-production of neurons and glia. Curr Opin Neurobiol 23: 1049-1056 Doi 10.1016/j.conb.2013.06.003

12 Faul M, Coronado V (2015) Epidemiology of traumatic brain injury. Handb Clin Neurol 127: 3-13 Doi 10.1016/B978-0-444-52892-6.00001-5

13 Felmingham KL, Baguley IJ, Green AM (2004) Effects of diffuse axonal injury on speed of information processing following severe traumatic brain injury. Neuropsychology 18: 564-571 Doi 10.1037/0894-4105.18.3.564

14 Ford MC, Alexandrova O, Cossell L, Stange-Marten A, Sinclair J, Kopp-Scheinpflug C, Pecka M, Attwell D, Grothe B (2015) Tuning of Ranvier node and internode properties in myelinated axons to adjust action potential timing. Nat Commun 6: 8073 Doi 10.1038/ncomms9073

15 Freeman SA, Desmazieres A, Fricker D, Lubetzki C, Sol-Foulon N (2016) Mechanisms of sodium channel clustering and its influence on axonal impulse conduction. Cell Mol Life Sci 73: 723-735 Doi 10.1007/s00018-015-2081-1

16 Gasser A, Ho TS, Cheng X, Chang KJ, Waxman SG, Rasband MN, Dib-Hajj SD (2012) An ankyrinG-binding motif is necessary and sufficient for targeting Nav1.6 sodium channels to axon initial segments and nodes of Ranvier. J Neurosci 32: 7232-7243 Doi 10.1523/JNEUROSCI.5434-11.2012

17 Iwata A, Stys PK, Wolf JA, Chen XH, Taylor AG, Meaney DF, Smith DH (2004) Traumatic axonal injury induces proteolytic cleavage of the voltage-gated sodium

channels modulated by tetrodotoxin and protease inhibitors. J Neurosci 24: 4605-4613 Doi 10.1523/JNEUROSCI.0515-03.2004
18 Jenkins SM, Bennett V (2002) Developing nodes of Ranvier are defined by ankyrin-G clustering and are independent of paranodal axoglial adhesion. Proc Natl Acad Sci U S A 99: 2303-2308 Doi 10.1073/pnas.042601799
19 Jette N, Coderre E, Nikolaeva MA, Enright PD, Iwata A, Smith DH, Jiang Q, Stys PK (2006) Spatiotemporal distribution of spectrin breakdown products induced by anoxia in adult rat optic nerve in vitro. J Cereb Blood Flow Metab 26: 777-786 Doi 10.1038/sj.jcbfm.9600226
20 Johnson VE, Meaney DF, Cullen DK, Smith DH (2015) Animal models of traumatic brain injury. Handb Clin Neurol 127: 115-128 Doi 10.1016/B978-0-444-52892-6.00008-8
21 Johnson VE, Stewart W, Smith DH (2013) Axonal pathology in traumatic brain injury. Exp Neurol 246: 35-43 Doi 10.1016/j.expneurol.2012.01.013
22 Johnson VE, Stewart W, Weber MT, Cullen DK, Siman R, Smith DH (2016) SNTF immunostaining reveals previously undetected axonal pathology in traumatic brain injury. Acta Neuropathol 131: 115-135 Doi 10.1007/s00401-015-1506-0
23 Johnson VE, Weber MT, Xiao R, Cullen DK, Meaney DF, Stewart W, Smith DH (2018) Mechanical disruption of the blood-brain barrier following experimental concussion. Acta Neuropathol 135: 711-726 Doi 10.1007/s00401-018-1824-0
24 Kourtidou P, McCauley SR, Bigler ED, Traipe E, Wu TC, Chu ZD, Hunter JV, Li X, Levin HS, Wilde EA (2013) Centrum semiovale and corpus callosum integrity in relation to information processing speed in patients with severe traumatic brain injury. J Head Trauma Rehabil 28: 433-441 Doi 10.1097/HTR.0b013e3182585d06
25 Kushner D (1998) Mild Traumatic Brain Injury: Toward Understanding Manifestations and Treatment. Archives of Internal Medicine 158: 1617-1624 Doi 10.1001/archinte.158.15.1617
26 Labasque M, Devaux JJ, Leveque C, Faivre-Sarrailh C (2011) Fibronectin type III-like domains of neurofascin-186 protein mediate gliomedin binding and its clustering at the developing nodes of Ranvier. J Biol Chem 286: 42426-42434 Doi 10.1074/jbc.M111.266353
27 Liu CH, Rasband MN (2019) Axonal Spectrins: Nanoscale Organization, Functional Domains and Spectrinopathies. Front Cell Neurosci 13: 234 Doi 10.3389/fncel.2019.00234
28 Marion CM, Radomski KL, Cramer NP, Galdzicki Z, Armstrong RC (2018) Experimental Traumatic Brain Injury Identifies Distinct Early and Late Phase Axonal Conduction Deficits of White Matter Pathophysiology, and Reveals Intervening Recovery. J Neurosci 38: 8723-8736 Doi 10.1523/JNEUROSCI.0819-18.2018
29 Meaney DF, Smith DH (2011) Biomechanics of concussion. Clin Sports Med 30: 19-31, vii Doi 10.1016/j.csm.2010.08.009
30 Palacios EM, Owen JP, Yuh EL, Wang MB, Vassar MJ, Ferguson AR, Diaz-Arrastia R, Giacino JT, Okonkwo DO, Robertson CSet al (2020) The evolution of white matter microstructural changes after mild traumatic brain injury: A longitudinal DTI and NODDI study. Sci Adv 6: eaaz6892 Doi 10.1126/sciadv.aaz6892
31 Pfister BJ, Bonislawski DP, Smith DH, Cohen AS (2006) Stretch-grown axons retain the ability to transmit active electrical signals. FEBS Lett 580: 3525-3531 Doi 10.1016/j.febslet.2006.05.030
32 Rabinowitz AR, Smith DH (2016) Chapter 9 - Traumatic Brain Injury and Rationale for a Neuropsychological Diagnosis of Diffuse Axonal Injury. In: Lazarov O, Tesco G (eds) Genes, Environment and Alzheimer's Disease. Academic Press, City, pp 267-293
33 Raghavan M, Fee D, Barkhaus PE (2019) Generation and propagation of the action potential. Handb Clin Neurol 160: 3-22 Doi 10.1016/B978-0-444-64032-1.00001-1

34 Rasband MN, Peles E (2021) Mechanisms of node of Ranvier assembly. Nat Rev Neurosci 22: 7-20 Doi 10.1038/s41583-020-00406-8
35 Rasband MN, Peles E (2015) The Nodes of Ranvier: Molecular Assembly and Maintenance. Cold Spring Harb Perspect Biol 8: a020495 Doi 10.1101/cshperspect.a020495
36 Reeves TM, Greer JE, Vanderveer AS, Phillips LL (2010) Proteolysis of submembrane cytoskeletal proteins ankyrin-G and alphaII-spectrin following diffuse brain injury: a role in white matter vulnerability at Nodes of Ranvier. Brain Pathol 20: 1055-1068 Doi 10.1111/j.1750-3639.2010.00412.x
37 Reeves TM, Phillips LL, Povlishock JT (2005) Myelinated and unmyelinated axons of the corpus callosum differ in vulnerability and functional recovery following traumatic brain injury. Exp Neurol 196: 126-137 Doi 10.1016/j.expneurol.2005.07.014
38 Rios JC, Melendez-Vasquez CV, Einheber S, Lustig M, Grumet M, Hemperly J, Peles E, Salzer JL (2000) Contactin-associated protein (Caspr) and contactin form a complex that is targeted to the paranodal junctions during myelination. J Neurosci 20: 8354-8364
39 Royeck M, Horstmann MT, Remy S, Reitze M, Yaari Y, Beck H (2008) Role of axonal NaV1.6 sodium channels in action potential initiation of CA1 pyramidal neurons. J Neurophysiol 100: 2361-2380 Doi 10.1152/jn.90332.2008
40 Sherman DL, Tait S, Melrose S, Johnson R, Zonta B, Court FA, Macklin WB, Meek S, Smith AJ, Cottrell DFet al (2005) Neurofascins are required to establish axonal domains for saltatory conduction. Neuron 48: 737-742 Doi 10.1016/j.neuron.2005.10.019
41 Smith DH, Stewart W (2020) 'Concussion' is not a true diagnosis. Nat Rev Neurol 16: 457-458 Doi 10.1038/s41582-020-0382-y
42 Susuki K (2013) Node of Ranvier disruption as a cause of neurological diseases. ASN Neuro 5: 209-219 Doi 10.1042/AN20130025
43 von Reyn CR, Mott RE, Siman R, Smith DH, Meaney DF (2012) Mechanisms of calpain mediated proteolysis of voltage gated sodium channel alpha-subunits following in vitro dynamic stretch injury. J Neurochem 121: 793-805 Doi 10.1111/j.1471-4159.2012.07735.x
44 von Reyn CR, Spaethling JM, Mesfin MN, Ma M, Neumar RW, Smith DH, Siman R, Meaney DF (2009) Calpain mediates proteolysis of the voltage-gated sodium channel alpha-subunit. J Neurosci 29: 10350-10356 Doi 10.1523/JNEUROSCI.2339-09.2009
45 Wolf JA, Johnson BN, Johnson VE, Putt ME, Browne KD, Mietus CJ, Brown DP, Wofford KL, Smith DH, Grady MSet al (2017) Concussion Induces Hippocampal Circuitry Disruption in Swine. J Neurotrauma 34: 2303-2314 Doi 10.1089/neu.2016.4848
46 Yuen TJ, Browne KD, Iwata A, Smith DH (2009) Sodium channelopathy induced by mild axonal trauma worsens outcome after a repeat injury. J Neurosci Res 87: 3620-3625 Doi 10.1002/jnr.22161

Tables and Figure legends

Table 1. Summary of antibodies used for IHC and IF.

Antibody	Epitope	Type	Dilution	Company
APP	N-terminal aa 66-81, clone 22C11	Mouse, Monoclonal	1:80,000 for IHC and 1:8,000 for IF	Millipore Sigma
Nav1.6	aa 1042-1061 of rat Nav1.6	Rabbit, Polyclonal	1:200 for IF	Alomone
Caspr	Generated against a glutathione S-transferase (GST) fusion protein composed of the entire cytoplasmic domain of rat p190/Caspr (GST-190CT).	Guinea pig	1:1,000 for IF	From Stephen Waxman
βIV-spectrin	N-terminal aa 15-38	Rabbit	1:1,000 for IF	From Matthew Rasband
AnkG	N106/36, fusion protein ~1000 amino acids of Ankyrin-G	Mouse, Monoclonal	1:1000 for IF	NeuroMab
Nfasc	C-terminus	Rabbit	1:2,000 for IF	From Peter Brophy

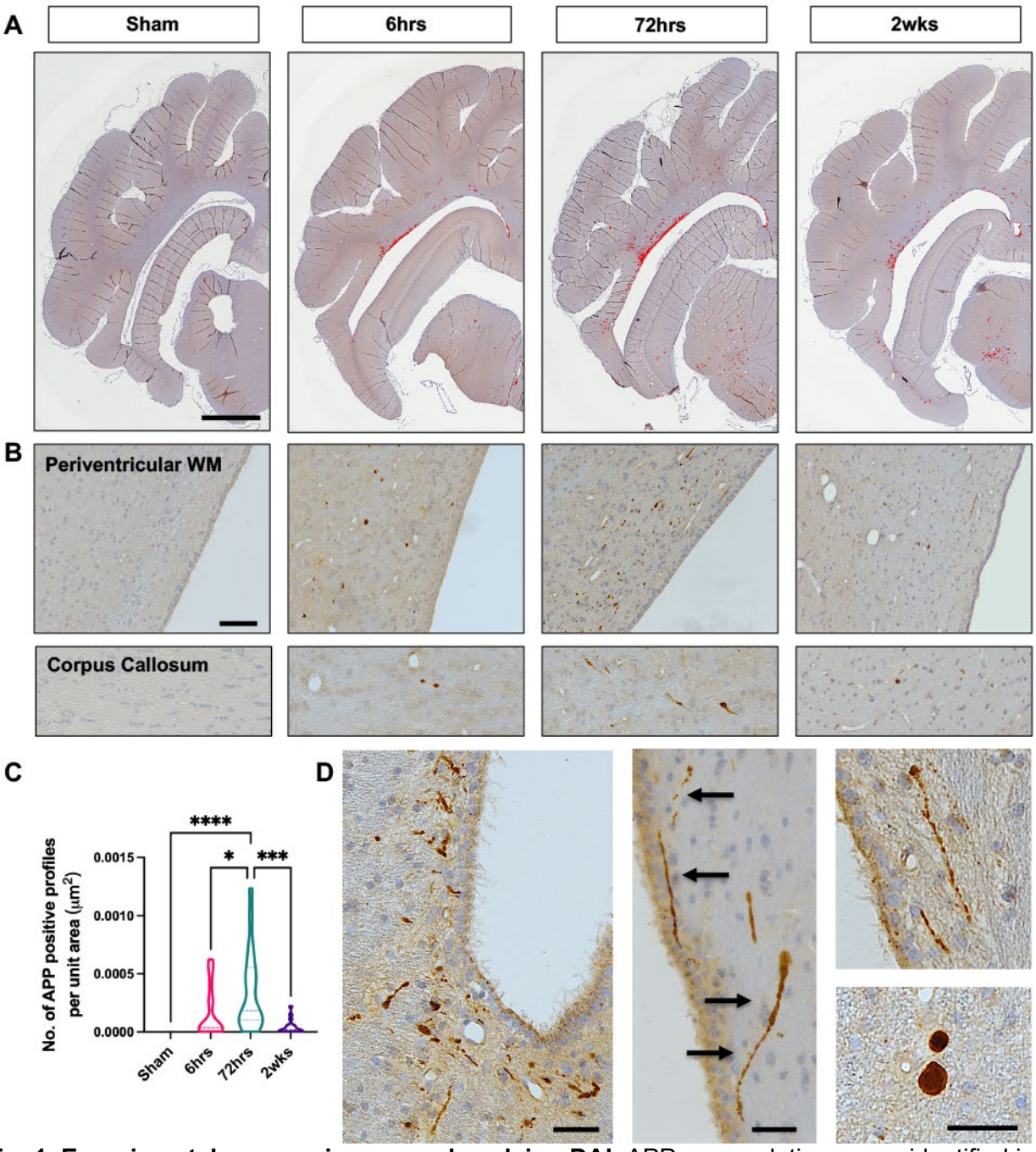

Fig. 1. Experimental concussion caused evolving DAI. APP accumulations were identified in injured axons from 6hrs to 2wks after rotational acceleration injury in swine. A) Whole slide imaging revealed progression of DAI (red dots represented APP positive swollen profiles, scale bar = 5 mm). B) Representative images of periventricular white matter and corpus callosum APP profiles were shown (scale bar = 50 μm). C) Increases of the average number of APP positive profiles per unit area (μm^2) were found after injury at all time points. 72hrs post injury appeared to show peak numbers of APP positive profiles. D) Various swollen axonal profiles were displayed, including terminal swelling, beading, and fusiform profiles (left two columns and upper right panel, scale bar = 25 μm). Such injured morphologies suggest transport interruption caused by DAI. Further, extensive APP axonal bulbs were identified at periventricular white matter (lower right panel).

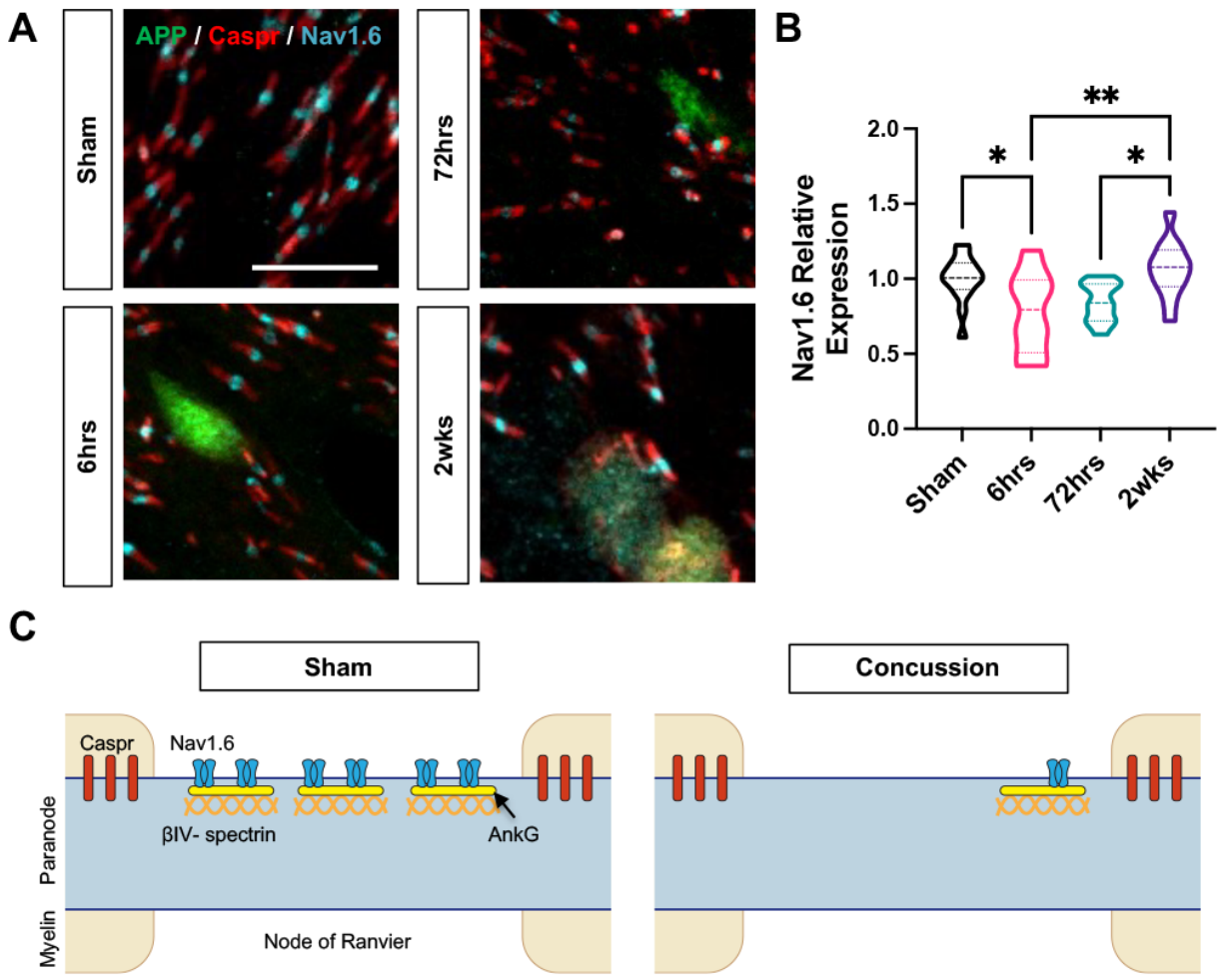

Fig. 2. Widespread changes in Nav1.6 associated with DAI. A) Experimental concussion led to white matter (periventricular) Nav1.6 changes relevant to DAI, as evidenced by APP IF staining. Co-staining of Nav1.6 and Caspr were used to illustrate NOR and paranode, respectively (scale bar = 10 μm). B) Nav1.6 relative expression levels were found significantly reduced at 6hrs post injury as compared to sham control, while gradually returned after 2wks of injury. C) Scheme showing acute downregulation of Nav1.6 after concussion, as compared to sham (light brown represents myelin, light blue-axon, red-Caspr, medium blue-Nav1.6, yellow-AnkG, orange-βIV-spectrin). Nav1.6 was anchored on NOR cytoskeleton scaffold of AnkG and βIV-spectrin. Paranode space was filled with Caspr immunoreactivity.

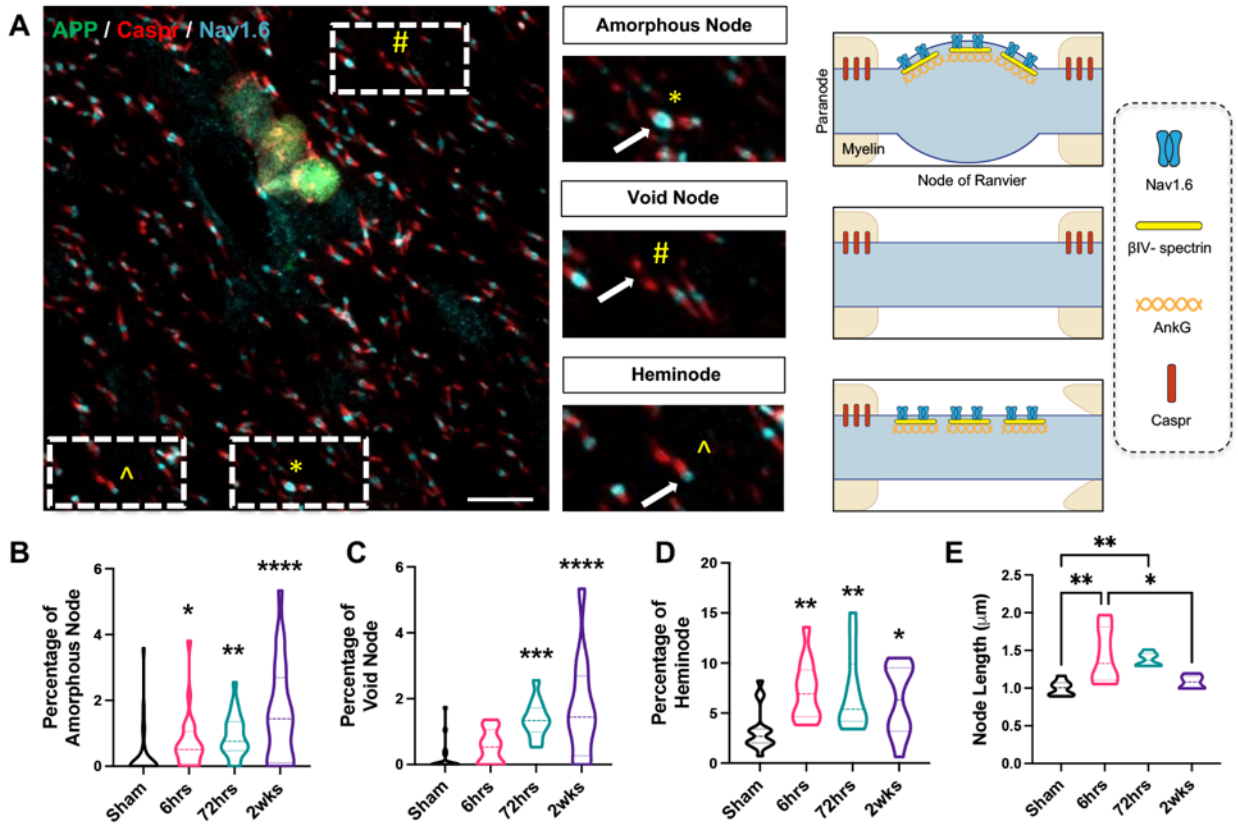

Fig. 3. Progressive disruption of NOR integrity after injury. A) Changes in NOR morphologies were captured at 2wks post injury. Representative amorphous, void, and heminode were shown (indicated by the white arrow, scale bar = 10 μm), accompanied with schemes showing individual NOR changes (light brown represents myelin, light blue-axon, red-Caspr, medium blue-Nav1.6, yellow-AnkG, orange-βIV-spectrin). B-D) Percentage of amorphous, void, and heminode were all significantly increased at various time points post injury. E) Significant elevations of node lengths (gap size) were identified both at 6hrs and 72hrs post injury.

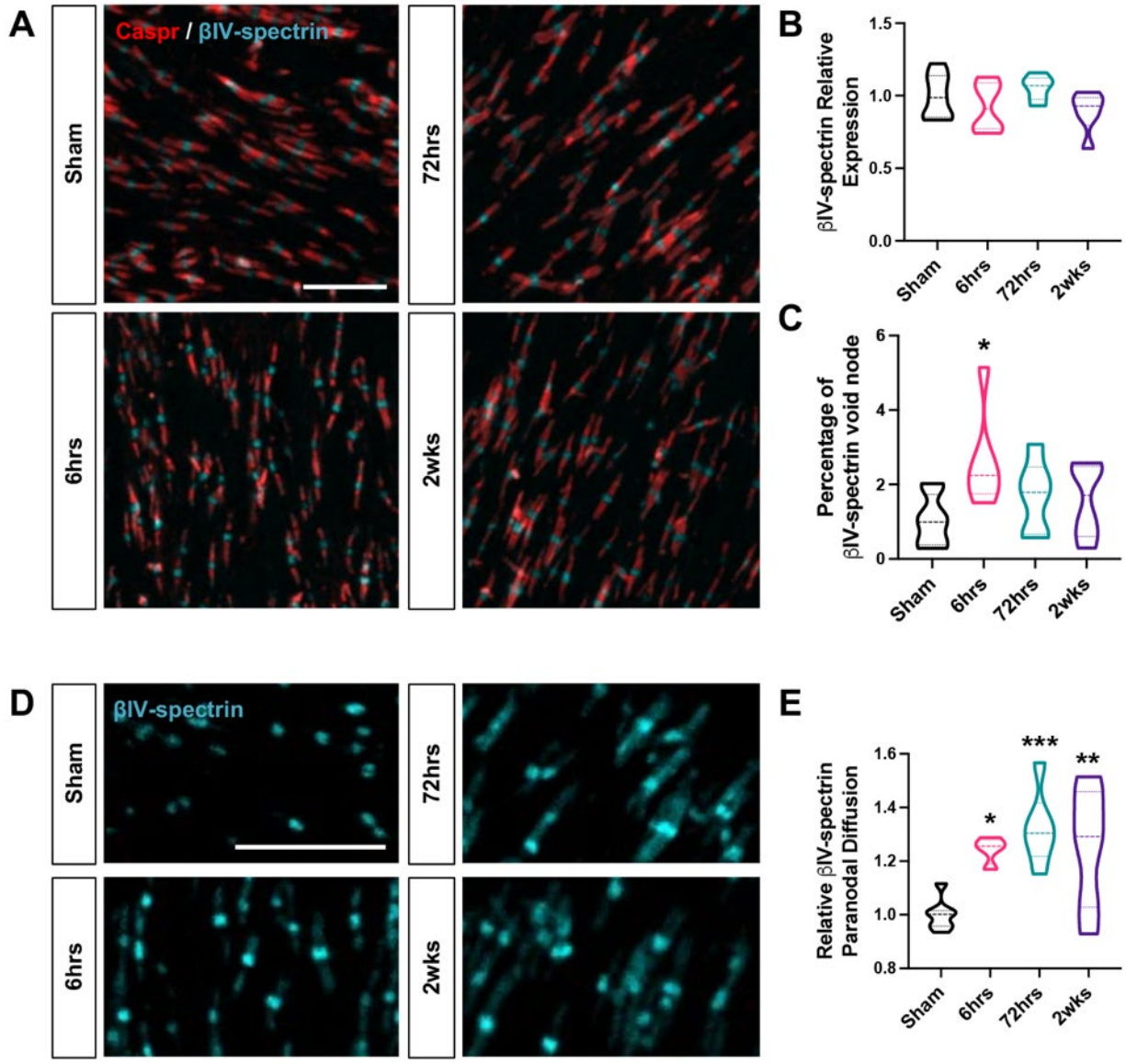

Fig. 4. Diffusion of βIV-spectrin into paranodal space after injury. A) IF staining showed βIV-spectrin positive NOR along with Caspr labeled paranodal space within white matter (scale bar = 10 μm). B-C) While no change in βIV-spectrin expression level within the nodal gap was found, a significant increase in percentage of βIV-spectrin void node was identified at 6hrs post injury. D-E) Significant diffusions of βIV-spectrin staining into the paranodal space were evident from 6hrs to 2wks post injury (scale bar = 10 μm).

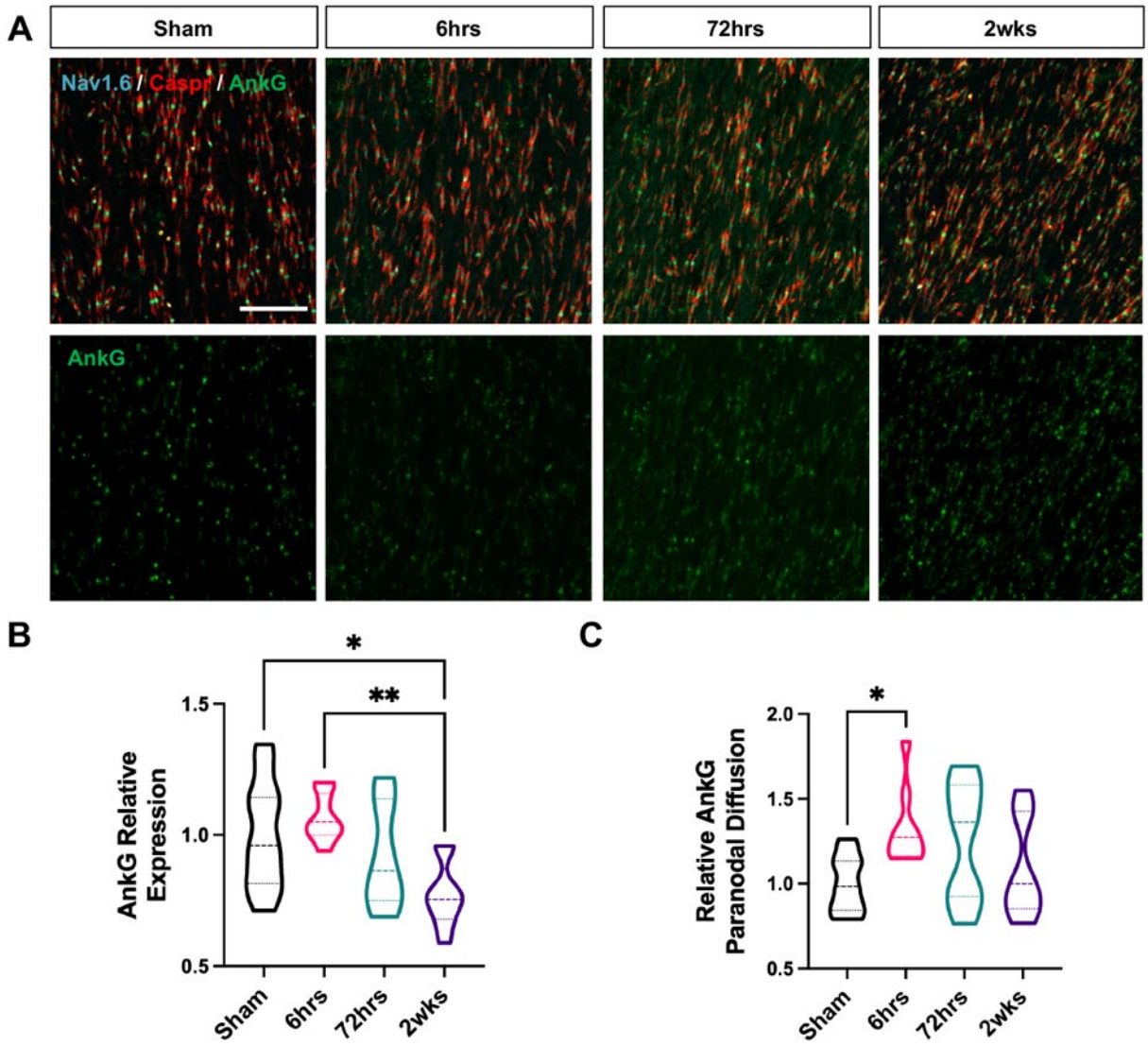

Fig. 5. Changes in AnkG expression and concurrent diffusion into paranodal space after injury. A) Representative images showing decreases in AnkG IF staining after concussion with progressive increased paranodal diffusion (scale bar = 20 μm). B) Significant decrease of AnkG expression at NOR was observed at 2wks post injury. C) Significant diffusion of AnkG into paranodal space was observed at 6hrs post injury.

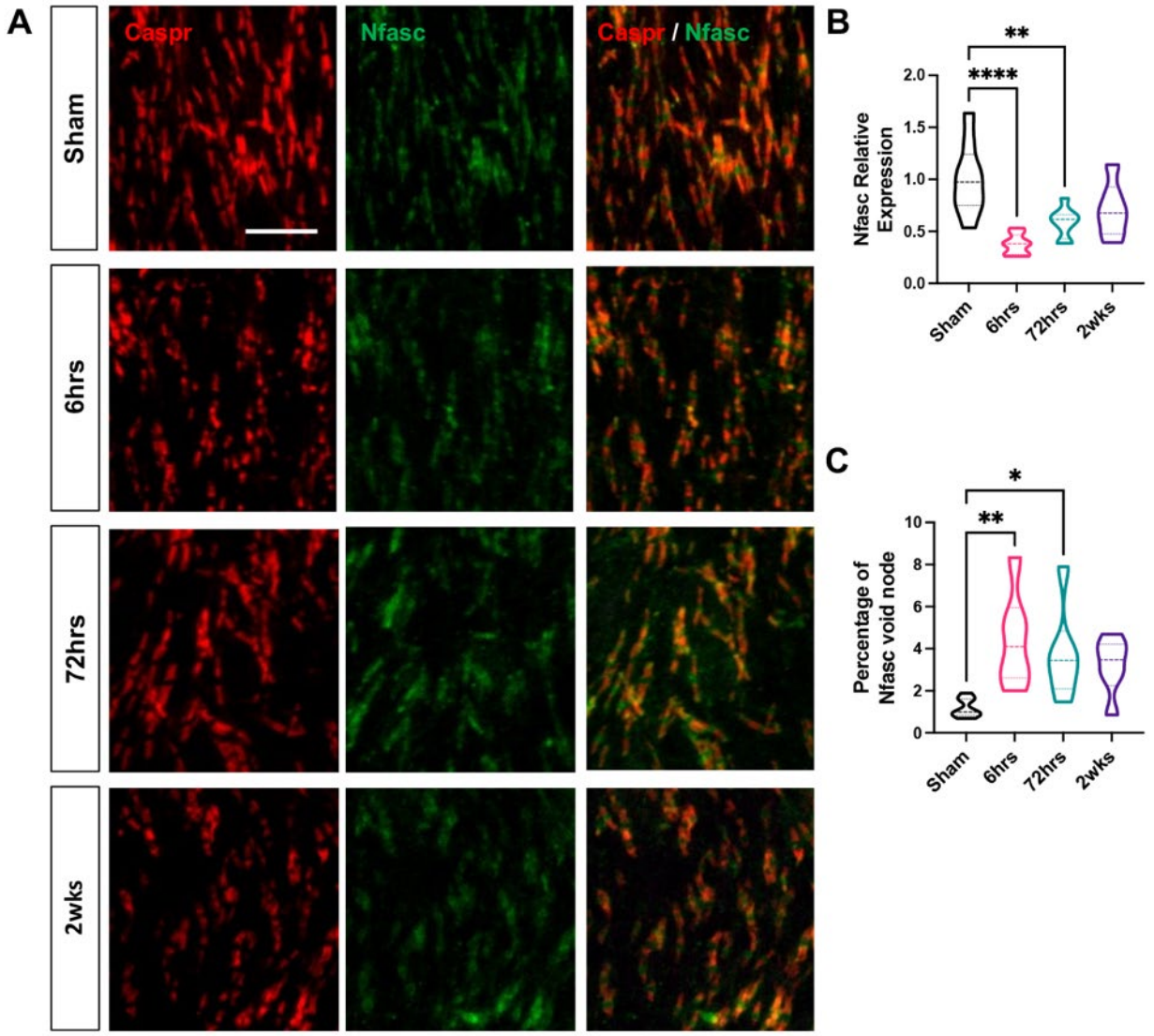

Fig. 6. Persistent loss of Nfasc profiles relevant to NOR. A) Co-staining of Caspr and Nfasc showed both NOR and paranodal space within white matter (scale bar = 10 μm). B) Significant loss of Nfasc expressions were identified at 6hrs and 72hrs post injury, while a trend decrease was seen at 2wks time point. C) Similarly, sustained increases of percentage of Nfasc void node were found.

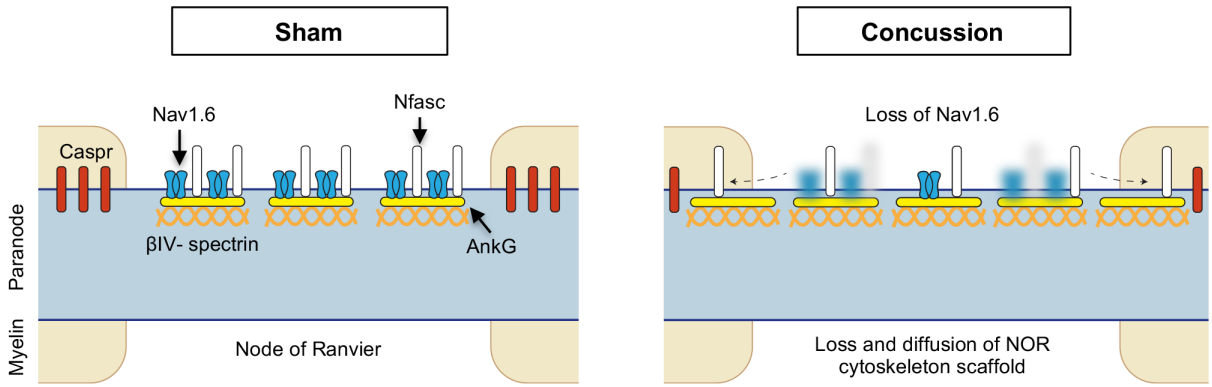

Fig. 7. A scheme depicting widespread changes of Nav1.6 and disruption of NOR cytoskeleton scaffold after concussion. In sham animal (left panel), Nav1.6 and cytoskeleton scaffold proteins, including βIV-spectrin, AnkG, and Nfasc, are enriched in the NOR with Caspr presented in the paranodal space (light brown represents myelin, light blue-axon, red-Caspr, medium blue-Nav1.6, yellow-AnkG, orange-βIV-spectrin, white-Nfasc). However, after concussion, Nav1.6 expression is reduced within NOR, concurrent with evident loss and diffusion of βIV-spectrin, AnkG, and Nfasc into the paranodal space. Together, experimental concussion caused progressive loss and diffusion of NOR cytoskeleton scaffold, representing a unique phenotype of axonal pathology.